Ж У Р Н А Л   С Т Р У К Т У Р Н О Й   Х И М И И

2014. Том 55, № 3 *Май – июнь* *С. 469 – 475*

UDC 541.6:548.737:543.422

VIBRATIONAL SPECTROSCOPIC INVESTIGATION OF METHYL(5-[2-THIENYLCARBONYL]-1H-BENZIMIDAZOL-2-YL: A COMPARATIVE DENSITY FUNCTIONAL STUDY

Ö. Alver[1,2], C. Parlak[3], M. Fatih Kaya[3], G. Dikmen[1,2], L. Genç[2,4]

[1]*Department of Physics, Science Faculty, Anadolu University, Eskişehir, Turkey*
[2]*Plant, Drug and Scientific Research Centre, Anadolu University, Eskisehir, Turkey*
[3]*Department of Physics, Dumlupı nar University, Kütahya, Turkey*
E-mail: cemal.parlak@dpu.edu.tr
[4]*Department of Pharmaceutical Technology, Anadolu University, Eskişehir, Turkey*

Received November, 22, 2012

FT-IR and Raman spectra of methyl(5-[2-thienylcarbonyl]-1H-benzimidazol-2-yl (nocodazole) are experimentally examined in the region of 4000—400 cm^{-1}. The optimized geometric parameters, conformational equilibria, normal mode frequencies, and corresponding vibrational assignments of nocodazole ($C_{14}H_{11}N_3O_3S$) calculated by means of the B3LYP hybrid density functional theory (DFT) method using the 6-31++G(*d,p*) basis set. Vibrational assignments are made based on the total energy distribution (TED) and the thermodynamic functions, highest occupied and lowest unoccupied molecular orbitals (HOMO and LUMO) of nocodazole are calculated. Calculations are employed for four energetically possible conformers of nocodazole (N1, N2, N3 and N4) in the gas phase. A comparison between the experimental and theoretical results indicates that the B3LYP method is able to provide satisfactory results for predicting vibrational wavenumbers if calculated values are scaled properly and the structural parameters.

Keywords: nocodazole, vibrational spectra, TED, DFT, SQM.

INTRODUCTION

Nocodazole has been widely employed as an effective microtubule-disrupting agent and in many recent studies it has been used as for the activation of spindle checkpoint [1]. Indirectly acting mutagens are likely to exhibit a biological threshold as shown for microtubuledepolymerising chemicals such as colchicine, vinblastine, beno myl or nocodazole. Nocodazole even at very low concentrations is a classical aneugen which binds to beta-tubulin with high affinity and affects polymerisation kinetics. In addition, chemicals like colchicine or nocodazole may change the morphology of centromeres and kinetochores, the sites of attachment for spindle microtubules on the chromosome, and induce malorientation and lagging of chromosomes in mitotic and meiotic cells. Nocodazole is extensively used in cancer treatments [2—4].

The DFT/B3LYP model shows fairly good performance on electron affinities, bond energies and reasonably good performance on vibrational wavenumbers and geometric structures of organic compounds [5—13]. Even though, nocodazole has a wide range of potential applications, to the best of our knowledge, there is limited information available in the literature about its spectroscopic properties. For that reason, in the present study, a detailed quantum chemical investigation is performed to make definitive assignments to the fundamental normal modes of nocodazole and to clarify the ob-

---

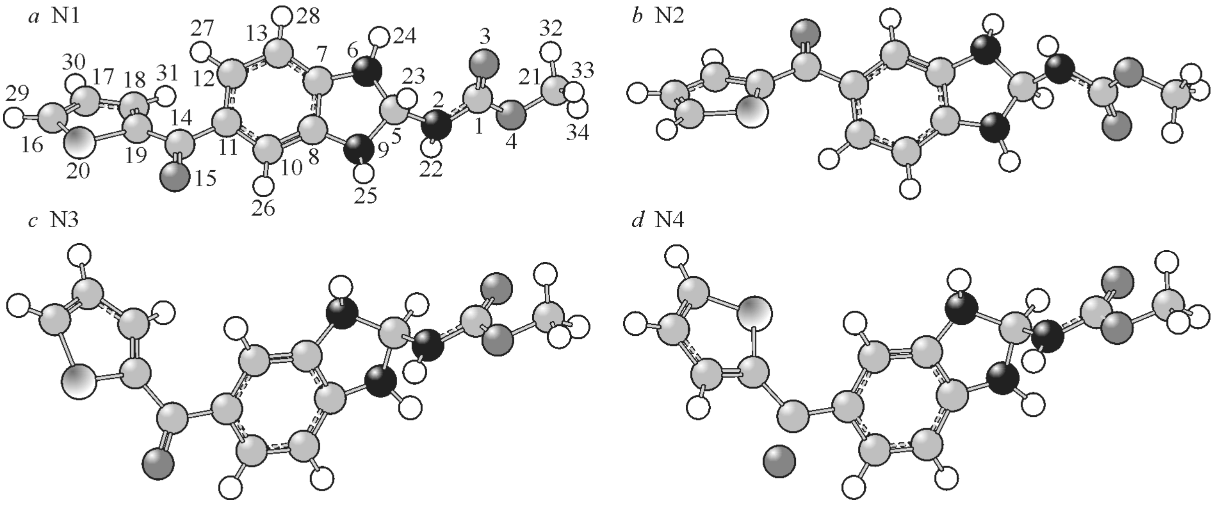

Fig. 1. Theoretically optimized four possible geometric structures with atom numbering of nocodazole; *a*) N1, *b*) N2, *c*) N3 and *d*) N4

tained experimental data for this molecule. The detailed results of the theoretical and spectroscopic studies are reported here. Additionally, vibrational spectra of nocodazole with TED data and structural parameters have been calculated for the most stable conformer in the gas phase at the B3LYP/6-31++G(*d*,*p*) level.

EXPERIMENTAL

A commercial sample of nocodazole was purchased (Acros Organics, ≥ % 98) and used without further purification. FT-IR spectra were recorded in the region with a Bruker Optics IFS66v/s FTIR spectrometer with a resolution of 2 cm^{-1}. The Raman spectrum was obtained using a Bruker Senterra Dispersive Raman microscope spectrometer with 785 nm excitation from a 3B diode laser having 3 cm^{-1} resolution.

CALCULATIONS

In order to determine the possible stable configurations, first, the conformational space of nocodazole was scanned with a semi-empirical calculation. This calculation was performed with the Spartan 10 program [14]. In the second step, calculations were performed using the Gaussian 09.A1 program [15]. GaussView 5.0.8 [16] was used for the visualization of the structure and simulated vibrational spectra. Within the possible conformers of nocodazole obtained with Spartan 10 (Fig. S1), four of them are likely to be present in amount enough for comparison. The rest of them seem energetically not possible. Henceforth, the investigation was limited to optimized N1, N2, N3, and N4 conformers as given in Fig. 1. For the calculations, all four forms of nocodazole were first optimized by B3LYP with the 6-31++G(*d*,*p*) basis set in the gas phase. Vibrational wavenumbers were calculated using the same method and basis set and then scaled by 0.955 (above 1800 cm^{-1}), 0.977 (under 1800 cm^{-1}), and using the SQM method for 6-31++G(*d*,*p*) [17—19]. The calculations gave no imaginary wavenumbers and confirmed that the optimization was successfully performed. TED calculations were carried out using the SQM method to describe the relative contributions of the redundant internal coordinates to each normal vibrational mode of the molecule [18, 19].

RESULTS AND DISCUSSION

The results of the calculations on the molecular conformations and structural parameters of nocodazole are discussed first. A brief discussion of the experimental and theoretical vibrational wavenumbers with the corresponding TED assignments and intensities is then presented.

GEOMETRIC STRUCTURES

Mole fractions of N1, N2, N3, and N4 conformers are calculated as 64 %, 21 %, 12 %, and 3 %. Based on the calculations, the N1 conformer is the most stable and abundant conformer in the gas phase and so approximate mode descriptions were made using the N1 conformer (Fig. 1, *a*).

For the optimized geometric parameters, the magnitude of dihedral angles D(6; 7; 8; 9) = 0.34°, D(6; 7; 13; 12) = 177.66°, D(6; 7; 8; 10) = 178.51°, D(8; 10; 11; 12) = 0.97°, D(6; 7; 13; 28) = 3.34°, D(12; 11; 10; 26) = 178.24°, D(8; 10; 11; 14) = 177.09° indicate that all carbon, nitrogen, and hydrogen atoms presented above are nearly on the same plane. The carbon atom indicated with number 5 is the apex of the envelope constructed by N(6), C(7), C(8), N(9), and C(5) atoms and the corresponding dihedral angle for D(8; 9; 5; 23) is 100.34°, which indicates that H(23) is almost axial to the plane constructed by N(6), C(7), C(8), and N(9) atoms. The S—C bond length, C—S—C, S—C—H, and C—C—H bond angles of thiophene were previously reported as 1.7140 Å, 92.17°, 119.85°, and 123.28° respectively [20]. In this study, S(20)—C(19) and S(20)—C(16) bond lengths were calculated as 1.7490 Å and 1.7258 Å respectively. C(19)—S(20)—C(16), S(20)—C(16)—H(29), and C(16)—C(17)—H(30) bond angles were calculated as 91.43°, 120.01°, and 123.66° respectively. Reported values seem to be in agreement with the previously reported data.

VIBRATIONAL STUDIES OF NOCODAZOLE

Based on the literature survey, to the best of our knowledge, no vibrational wavenumbers and assignments of nocodazole in the region of 4000—400 cm^{-1} have been reported yet. The measured and calculated vibrational wavenumbers along with the corresponding vibrational assignments and intensities and the theoretical-experimental vibrational spectra of nocodazole are given in Table 1 and Figs. 2, 3 respectively.

The nocodazole molecule consists of 34 atoms, so it has 96 normal vibrational modes and its most stable form belongs to the point group C_1 with the only identity (E) symmetry element or operation. The TED assignments for the vibrational modes of nocodazole have been provided by SQM [18, 19] in Table 1. According to the calculations, 19 normal vibrational modes of nocodazole are below 400 cm^{-1}. The high wavenumber region, the strong broad NH stretching in the title molecule is assigned to

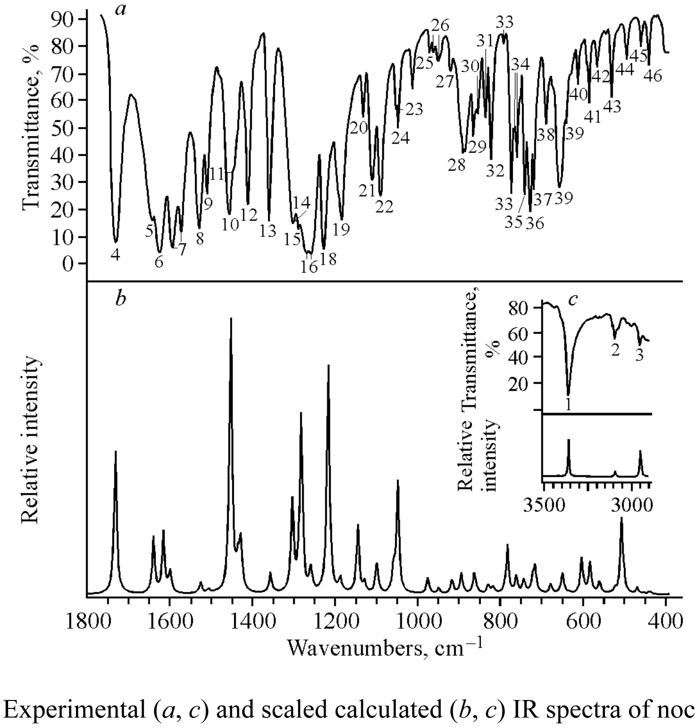

Fig. 2. Experimental (*a*, *c*) and scaled calculated (*b*, *c*) IR spectra of nocodazole

Table 1

Vibrational frequencies (cm^{-1}) *and* TED *assignments of the* N1 *conformer for nocodazole*

Mode	TED (≥ 7 %)	Experimental		B3LYP/6-31++G(*d,p*)				
				N1 conformer in the gas phase				
		IR	Raman	ν^{α}	ν^{β}	ν^{φ}	I_{IR}	I_{R}
1	2	3	4	5	6	7	8	9
ν_1	ν 24-6 (99)	3361	—	3620	3457	3361	61.85	4.73
ν_2	ν 30-17 (75) + ν 31-18 (14) + ν 27-12 (6)	3094	—	3219	3074	3094	9.37	3.82
ν_3	ν 32-21 (40) + ν 33-21 (39) + ν 34-21 (20)	2947	—	3066	2928	2947	45.78	5.39
ν_4	ν 3-1 (79)+ ν 2-1 (8)	1731	—	1777	1736	1732	332.33	0.64
ν_5	ν 15-14 (68)+ ν 10-8 (7)	1643	1636	1683	1644	1640	130.72	30.52
ν_6	ν 10-8 (31) + ν 15-14 (14) + ν 13-12 (8) + + ν 12-11 (7) + ν 8-7 (7)	1625	—	1657	1619	1616	143.16	62.00
ν_7	ν 13-7 (30) + ν 8-7 (12) + ν 12-11 (11) + ν 15-14 (9)	1595 1574	1607 1581	1640	1602	1600	47.68	9.90
ν_8	ν 19-18 (35)+ ν 17-16 (22)+ δ 31-18-17 (11) + + δ 18-17-30 (8)	1529	—	1563	1526	1526	25.17	2.25
ν_9	ν 8-7 (11) + ν 7-6 (8)+ δ 28-13-7 (7)	1510	—	1540	1504	1506	9.42	3.41
ν_{10}	δ 32-21-33 (54) + τ 33-21-4-1 (8) τ 32-21-4-1 (7) + δ 32-21-4 (7)	1455	—	1495	1461	1453	631.45	33.98
ν_{11}	δ 24-6-5 (10) + δ 32-21-34 (9)	1444	—	1472	1438	1436	58.69	4.64
ν_{12}	ν 17-16 (21) + ν 18-17 (14)+ ν 19-18 (10) + + δ 32-21-34 (7)	1411	1423	1465	1431	1429	108.79	60.17
ν_{13}	δ 17-16-29 (18)+ δ 20-16-29 (13)+ ν 17-16 (12) ν 19-18 (12) + ν 18-17 (11) + δ 30-17-16 (10)	1360	1364	1385	1353	1357	47.46	3.02
ν_{14}	δ 7-6-24 (8) + ν 12-11 (7)	1301	1296	1328	1297	1304	207.08	5.02
ν_{15}	ν 14-11 (24) + ν 19-14 (13) + δ 13-12-27 (9)	1290	—	1313	1283	1283	411.55	4.77
ν_{16}	ν 7-6 (20) + ν 13-12 (12) + δ 28-13-12 (10) δ 7-6-24 (10) + δ 28-13-7 (8)	1268 1258	1273	1285	1255	1259	52.57	2.18
ν_{17}	δ 26-10-8 (13) + δ 11-10-26 (11) + δ 19-18-31 (10) ν 19-18 (7)		1238	1250	1221	1226	74.98	4.57
ν_{18}	ν 4-1 (25)+ ν 2-1 (13) + δ 5-2-22 (13) + δ 22-2-1 (11)	1228	—	1245	1216	1217	525.27	0.73
ν_{19}	ν 9-8 (16) + ν 7-6 (8) + δ 28-13-7 (7)	1184	—	1214	1186	1188	31.93	0.72
ν_{20}	ν 5-2 (47) + ν 21-4 (8)	1132	1140	1173	1146	1146	158.77	1.01
ν_{21}	ν 13-12 (22) + δ 28-13-12 (17) + δ 27-12-11 (10) δ 13-12-27 (8)	1110	1118	1153	1126	1129	23.26	0.73
ν_{22}	δ 18-17-30 (10) + δ 30-17-16 (8) + δ 17-16-29 (8) δ 11-10-26 (7) + ν 14-11 (7) + ν 17-16 (7)	1089	1090	1124	1098	1100	69.08	6.06
ν_{23}	ν 9-5 (30) + ν 6-5 (19)	1052	—	1085	1060	1059	44.04	1.84
ν_{24}	ν 18-17 (26) + δ 31-18-17 (14)	1047	1036	1074	1049	1049	256.74	0.97
ν_{25}	ν 6-5 (27) + ν 21-4 (12)	970	966	998	975	976	35.77	2.43
ν_{26}	ν 21-4 (9) + ν 11-10 (9) + ν 9-8 (7) + δ13 -12-11 (7)	961 950	—	973	951	950	13.47	4.43
ν_{27}	ν 21-4 (19) + ν 6-5 (17) + ν 9-5 (13) + ν 4-1 (12)	920	—	941	919	918	31.12	1.02
ν_{28}	τ 26-10-8-9 (25) + τ 14-11-10-26 (25) τ 26-10-8-7 (17) + τ 12-11-10-26 (14)	890	—	903	882	895	49.03	4.38

Continued Table 1

1	2	3	4	5	6	7	8	9
ν_{29}	ν 8-7 (17)+ δ 6-5-9 (8)	864	873	881	861	864	47.78	14.46
ν_{30}	ν 20-16 (15) + δ 17-16-20 (10)+ δ 18-17-16 (9) δ 20-16-29 (7)	855	—	878	858	857	5.42	2.97
ν_{31}	ν 20-16 (14) + τ 28-13-7-6 (9)+ τ 28-13-12-11 (7)	836	—	848	828	830	17.75	3.21
ν_{32}	τ 28-13-7-6 (14) + τ 28-13-12-11 (11) + + τ 28-13-7-8 (8) τ 7-13-12-27 (7) + τ 27-12-11-14 (7)	821	—	827	808	818	16.34	0.45
ν_{33}	ν 9-8 (8) + ν 8-7 (7)	791 774	—	803	784	784	113.39	0.73
ν_{34}	τ 5-2-1-3 (24) + τ 21-4-1-3 (22) + τ 22-2-1-3 (14) τ 22-2-1-4 (13)	766 759	762	778	760	762	40.43	0.03
ν_{35}	τ 15-14-11-10 (12) + τ 19-14-11-12 (11) τ 20-19-14-15 (9) + τ 18-19-14-11 (8)	740	744	762	744	744	31.13	3.72
ν_{36}	τ 18-17-16-29 (26) + τ 19-20-16-29 (20) τ 30-17-16-20 (12) + τ 19-18-17-30 (10)	727	—	733	716	723	30.17	0.25
ν_{37}	τ 10-8-7-13 (7) + τ 28-13-7-8 (7)	718	—	727	710	717	58.12	0.86
ν_{38}	ν 20-19 (13) + ν 19-14 (9) + ν 20-16 (8) + ν 19-18 (7)	688	701	719	702	679	23.30	0.55
*ν_{39}	δ 15-14-19 (6) + δ 8-7-6 (6)	656 640	658	666	651	651	49.21	2.49
ν_{40}	τ 25-9-5-2 (9)	611	—	617	603	604	84.12	3.48
*ν_{41}	τ 25-9-8-7 (6)	585	—	594	580	584	72.46	3.21
*ν_{42}	δ 2-1-4 (6)	565	573	575	562	561	28.13	3.58
ν_{43}	δ 19-14-11 (9) + ν 20-19 (7)	530	541	537	525	523	7.63	4.18
ν_{44}	τ 24-6-5-9 (19) + τ 13-7-6-24 (15) + τ 8-7-6-24 (15) τ 24-6-5-23 (7)	494	505	514	502	507	176.78	32.27
ν_{45}	τ 19-20-16-17 (8)	459	—	480	469	469	13.07	0
ν_{46}	τ 19-20-16-17 (9) + τ 16-20-19-18 (8)	441	—	451	441	440	6.23	0

Note. ν^{α}: Unscaled wavenumbers. ν^{β}: Scaled with 0.955 above 1800 cm^{-1}, 0.977 under 1800 cm^{-1}. ν^{φ}: Scaled by SQM methodology. IR and R: Calculated IR and Raman intensities. TED data are taken from SQM. *: TED (≥ 6 %).

3361 cm^{-1} in the IR spectrum and cannot be observed in the Raman spectrum. Possibly, this mode is Raman inactive for the experimental conditions previously discussed. The corresponding scaled theoretical values of this mode are 3457 cm^{-1} with 0.955 and 3361 cm^{-1} with SQM methodology with a 99 % TED contribution. The vibrational bands at 3094 cm^{-1}, 2947 cm^{-1} in the IR spectrum are due to CH and CH_3 stretching vibrations. These vibrations again are not present in the Raman spectrum, so, possibly they have low polarizability. The corresponding scaled calculated values for these bands were found as 3074 cm^{-1}, 2928 cm^{-1} with 0.955 and 3094 cm^{-1}, 2947 cm^{-1} with SQM methodology. Carbonyl stretching vibrations C(14)=O(15) and C(1)=O(3) appeared at 1731 cm^{-1}, 1643 cm^{-1} (IR) and 1636 cm^{-1} (R). C(1)O(3) has a very low Raman intensity compared to C(14)O(15), so it was not observed in the Raman spectrum (Fig. 3). The corresponding scaled calculated values for carbonyl stretching vibrations were found as 1777 cm^{-1}, 1683 cm^{-1} with 0.977 and 1732 cm^{-1}, 1640 cm^{-1} with SQM methodology. TED contributions of these bands to the related vibrational modes are 79 % and 68 % in the mentioned order (Table 1).

In the region of 1570—400 cm^{-1} a mixed type of vibrations including stretching, bending and torsions were revealed (Table 1). The CC, CN or CS stretching, CCC or CCH bending and some torsion

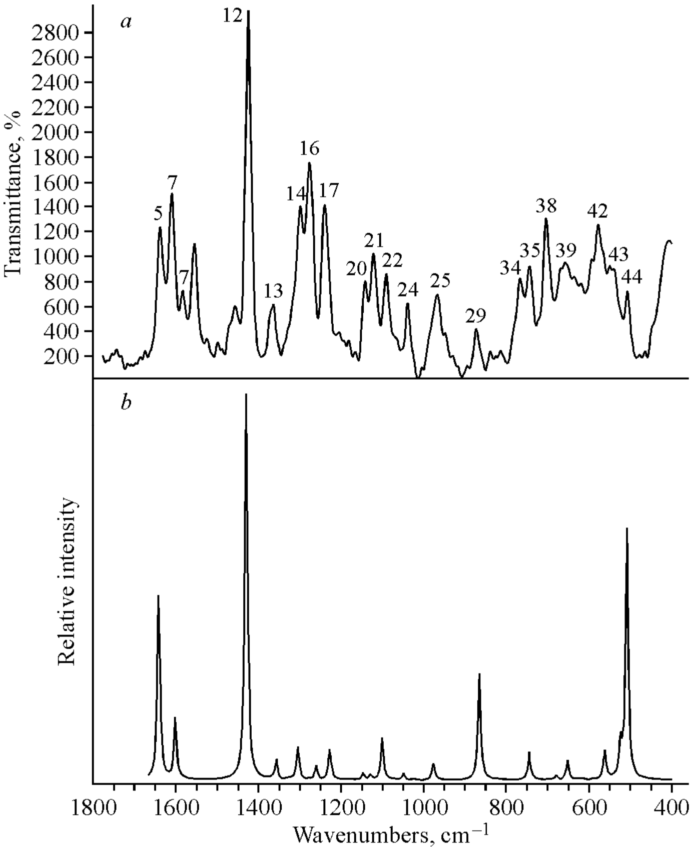

Fig. 3. Experimental (*a*) and scaled calculated (*b*) Raman spectra of nocodazole

modes dominate in the regions of 1000—400 cm^{-1}. The ν(C—N) stretching vibration of benzimidazole was reported by Vijayan et. al. as 1246 cm^{-1} (IR) and 1274 cm^{-1} (R) [20]. In the present work, it was experimentally observed at 1268/1258 cm^{-1} (IR) and 1274 cm^{-1} (R). The stretching vibration of N(6)—C(7) was calculated as 1255 cm^{-1} (with dual scaling) and 1259 cm^{-1} (with SQM) with 20 % TED contribution. Especially, under 900 cm^{-1}, torsions appeared in the calculated vibrational wavenumber. It is worth noting that, ν(S—C) stretching of thiophene was previously reported at around 840 cm^{-1} [21]. In this study, it has been found as 836 cm^{-1} and calculated as 828 cm^{-1} (with dual scaling) and 830 cm^{-1} (with SQM).

The calculated Raman activities are converted to relative Raman intensities using the following relationship derived from the intensity theory of Raman scattering:

$$I_i = f(\nu_0 - \nu_i)^4 S_i / \nu_i[1 - \exp(-hc\nu_i / kT)]$$

where ν_0 is the laser exciting wavenumbers in cm^{-1}, ν_i is the vibrational wavenumbers of the *i*th normal mode, S_i is the Raman scattering activity of the normal mode ν_i and *f* is a suitably chosen common normalization factor for all peak intensities, 10^{-14}; *h*, *k*, *c* and *T* are Planck and Boltzmann constants, speed of light, and temperature in Kelvin respectively [13, 22].

The HOMO and LUMO orbitals are the main orbitals for the chemical stability. The HOMO defines the ability to donate an electron and the LUMO as an electron acceptor. The absorption of the electronic transition is defined from the ground to the first excited state. The HOMO-LUMO energy gap from the ground state to the first excited state was calculated as around 3.72 eV. The laser used in this study for Raman measurements has an energy around half of this HOMO-LUMO gap. Therefore, the electronic excitement due to Raman laser seems not possible. The atomic compositions of frontier molecular orbital and their orbital energies are shown in Fig. 4.

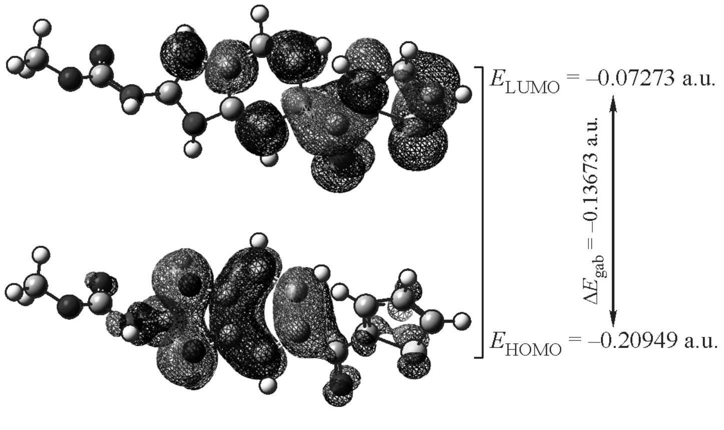

Fig. 4. Atomic orbital compositions of the frontier molecular orbital for nocodazole

CONCLUSIONS

The experimental and theoretical vibrational analysis of nocodazole has been performed and FT-IR and Raman spectra have been recorded in the range 4000—400 cm^{-1}. Various important vibrational bands have been discussed and assigned based on the calculated IR and Raman intensities. Some important structural parameters, IR and Raman wavenumbers and intensities of vibrational bands of nocodazole were calculated by DFT with the 6-31++G(*d,p*) basis set for the most stable conformer. To make a comparison with the experimental and calculated wavenumbers, we calculated root mean square deviation (rmsd) based on the calculation. The following rmsd values were obtained as 16.75 cm^{-1} (IR, 0.955/0.977), 7.02 cm^{-1} (IR, SQM), and 9.71 cm^{-1} (R, 0.955/0.977), 10.41 cm^{-1} (R, SQM). The correlation values between the experimental and calculated vibrational wavenumbers are found to be 0.99937 (IR) and 0.99923 (R) with 0.955—0.977 and 0.99988 (IR) and 0.99915 (R) with SQM. While SQM results seem far better in vibrational wavenumber calculations for IR, it is nearly the same for the Raman wavenumbers. Any differences observed between the experimental and calculated wavenumbers could be due to the fact that the calculations have been performed for a single isolated molecule in the gaseous state. The experimental values, however, were recorded in the presence of intermolecular interactions and increasing tendency to unharmonic vibrations in the high wavenumber region. In conclusion, the assignments made at the B3LYP/6-31++G(*d,p*) level of theory with only reasonable deviations from the experimental values seem understandable.

REFERENCES

1. *Cho S.G., Sihn C.R., Yoo S.J., Cho K.K., Lee H., Choi Y.J., Kim S.H.* // Cancer Lett. – 2006. – **241**. – P. 110 – 117.
2. *Shen Y., Betzendahl I., Sun F., Tinneberg H.R., Eichenlaub-Ritter U.* // Reprod. Toxicol. – 2005. – **19**. – P. 459 – 471.
3. *Marceiller J., Drechou A., Durand G., Perez F., Poqs C.* // Exp. Cell Res. – 2005. – **304**. – P. 483 – 492.
4. *Webb J.L., Ravikumar B., Rubinsztein D.C.* // Int. J. Biochem. Cell Biol. – 2004. – **36**. – P. 2541 – 2550.
5. *Scott A.P., Radom L.* // J. Phys. Chem. – 1996. – **100**. – P. 16502 – 16513.
6. *Ocola E.J., Brito T., McCann K., Laane J.* // J. Mol. Struct. – 2010. – **978**. – P. 74 – 78.
7. *Breda S., Reva I., Fausto R.* // J. Mol. Struct. – 2008. – **887**. – P. 75 – 86.
8. *Durig J.R., Ganguly A., El Defrawy A.M., Guirgis G.A., Gounev T.K., Herrebout W.A., Van Der Veken B.J.* // J. Mol. Struct. – 2009. – **918**. – P. 64 – 76.
9. *Yavuz M., Tanak H.* // J. Mol. Struct.: THEOCHEM. – 2010. – **961**, N 1-3. – P. 9 – 16.
10. *Parlak C.* // J. Mol. Struct. – 2010. – **966**. – P. 1 – 7.
11. *Rani U., Karabacak M., Tanrıverdi O., Kurt M., Sundaraganesan N.* // Spectrochim. Acta A. – 2012. – **92**. – P. 67.
12. *Alver Ö., Parlak C.* // J. Theor. Comput. Chem. – 2010. – **9**. – P. 667 – 685.
13. *Alver Ö., Parlak C.* // Vib. Spectroscop. – 2010. – **54**. – P. 1 – 9.
14. Spartan 10, Version 1.10, Wavefunction Inc., Irvine, CA 92612, USA, 2011.
15. *Frisch M.J., Trucks G.W., Schlegel H.B. et al.* Gaussian 09, Revision A.1, Gaussian Inc., Wallingford, CT, 2009.
16. *Dennington R.D., Keith T.A., Millam J.M.* GaussView, Version 5.0.8, Gaussian Inc., Wallingford, CT, 2008.
17. *Balcı K., Akyuz S.* // Vib. Spectroscop. – 2008. – **48**. – P. 215 – 228.
18. *Rauhut G., Pulay P.* // J. Phys. Chem. – 1995. – **99**. – P. 3093 – 3100.
19. *Baker J., Jarzecki A.A., Pulay P.* // J. Phys. Chem A. – 1998. – **102**. – P. 1412 – 1424.
20. *Vijayan N., Ramesh Babu R., Gopalakrishnan R., Ramasamy P., Harrison W.T.A.* // J. Crystal Growth. – 2004. – **262**. – P. 490 – 498.
21. *Kwiatkowski J.S., Leszczyński J., Teca I.* // J. Mol. Struct. – 1997. – **451**. – P. 436 – 437.
22. *Keresztury G., Holly S., Varga J., Besenyei G., Wang A.Y., Durig J.R.* // Spectrochim. Acta A. – 1993. – **49**. – P. 2007 – 2026.